NeuroImage: Clinical 23 (2019) 101899

Contents lists available at ScienceDirect

NeuroImage: Clinical

journal homepage: www.elsevier.com/locate/ynicl

Disrupted structural connectivity of fronto-deep gray matter pathways in progressive supranuclear palsy

Alexandra Abos[a], Barbara Segura[a,b], Hugo C. Baggio[a], Anna Campabadal[a], Carme Uribe[a], Alicia Garrido[c], Ana Camara[c], Esteban Muñoz[b,c,d], Francesc Valldeoriola[b,c,d], Maria Jose Marti[b,c,d], Carme Junque[a,b,d], Yaroslau Compta[b,c,d,*]

[a] Medical Psychology Unit, Department of Medicine, Institute of Neuroscience, University of Barcelona.Barcelona, Catalonia, Spain
[b] Centro de Investigación Biomédica en Red sobre Enfermedades Neurodegenerativas (CIBERNED), Hospital Clínic de Barcelona. Barcelona, Catalonia, Spain
[c] Movement Disorders Unit, Neurology Service, Hospital Clínic de Barcelona, Institute of Neuroscience, University of Barcelona, Barcelona, Catalonia, Spain
[d] Institute of Biomedical Research August Pi i Sunyer (IDIBAPS). Barcelona, Catalonia, Spain

ARTICLE INFO

Keywords:
Progressive supranuclear palsy
Structural connectivity
Tractography
Graph theory

ABSTRACT

Background: Structural connectivity is a promising methodology to detect patterns of neural network dysfunction in neurodegenerative diseases. This approach has not been tested in progressive supranuclear palsy (PSP).
Objectives: The aim of this study is reconstructing the structural connectome to characterize and detect the pathways of degeneration in PSP patients compared with healthy controls and their correlation with clinical features. The second objective is to assess the potential of structural connectivity measures to distinguish between PSP patients and healthy controls at the single-subject level.
Methods: Twenty healthy controls and 19 PSP patients underwent diffusion-weighted MRI with a 3T scanner. Structural connectivity, represented by number of streamlines, was derived from probabilistic tractography. Global and local network metrics were calculated based on graph theory.
Results: Reduced numbers of streamlines were predominantly found in connections between frontal areas and deep gray matter (DGM) structures in PSP compared with controls. Significant changes in structural connectivity correlated with clinical features in PSP patients. An abnormal small-world architecture was detected in the subnetwork comprising the frontal lobe and DGM structures in PSP patients. The classification procedure achieved an overall accuracy of 82.23% with 94.74% sensitivity and 70% specificity.
Conclusion: Our findings suggest that modelling the brain as a structural connectome is a useful method to detect changes in the organization and topology of white matter tracts in PSP patients. Secondly, measures of structural connectivity have the potential to correctly discriminate between PSP patients and healthy controls.

1. Introduction

Progressive supranuclear palsy (PSP) is a tauopathy characterized by a complex and heterogenic clinical presentation (Armstrong, 2018). In classical form (Richardson's syndrome), gait difficulty and falls are the most common initial manifestation and, as the disease progresses, other neurologic features appear, including dysphagia and dysarthria, eye movement abnormalities, parkinsonism and frontal cognitive dysfunction (Boxer et al., 2017).

Structural radiological features in PSP include atrophy of the midbrain, the middle and superior cerebellar peduncles (Price et al., 2004; Quattrone et al., 2008) and of deep gray matter structures, including the caudate, thalamus, putamen and hippocampus, and brainstem (Looi et al., 2011; Saini et al., 2013; Dąbrowska et al., 2015). Additionally, frontal cortical atrophy has also been consistently found (Cordato et al., 2000; Cordato et al., 2002; Brenneis et al., 2004). In line with the aforementioned, it has been hypothesized that clinical manifestations in PSP might result from the degeneration of deep gray matter structures, consequently disrupting cortico-subcortical brain circuits (Cummings, 1993; Litvan et al., 1996b; Cordato et al., 2005).

* Corresponding author at: Parkinson's Disease and Movement Disorders Unit of the Neurology Service of Hospital Clinic, Carrer de Villarroel 170, 08036 Barcelona, Catalonia, Spain.
E-mail addresses: alexandraabos@ub.edu (A. Abos), bsegura@ub.edu (B. Segura), hbaggio@ub.edu (H.C. Baggio), anna.campabadal@ub.edu (A. Campabadal), carme.uribe@ub.edu (C. Uribe), AGARRIDOP@clinic.cat (A. Garrido), ACAMARA@clinic.cat (A. Camara), JEMUNOZ@clinic.cat (E. Muñoz), fvallde@clinic.cat (F. Valldeoriola), mjmarti@clinic.cat (M.J. Marti), cjunque@ub.edu (C. Junque), YCOMPTA@clinic.cat (Y. Compta).

https://doi.org/10.1016/j.nicl.2019.101899
Received 12 March 2019; Received in revised form 9 June 2019
Available online 15 June 2019

Diffusion-weighted MRI (DWI) is a widely used technique to characterize the integrity of white matter (WM) tracts. In PSP, WM abnormalities have been predominantly found in the superior longitudinal fasciculus, corpus callosum and superior and middle cerebellar peduncles (Padovani et al., 2006; Whitwell et al., 2011a, 2011b; Surova et al., 2013, 2015; Agosta et al., 2014; Worker et al., 2014), along with deep gray matter structure involvement (Padovani et al., 2006; Wang et al., 2010; Whitwell et al., 2011a; Tsukamoto et al., 2012; Surova et al., 2015). Some studies also reported the contribution of WM alterations to clinical disease severity as well as performance in cognitive tests (Agosta et al., 2014; Surova et al., 2015; Wang et al., 2010; Whitwell et al., 2011b; Worker et al., 2014).

Tractography is an advanced DWI modality that allows reconstructing white matter fiber pathways of the brain and quantifying the local fiber density. The combination of tractography with graph theory has led to promising applications, as it can be used to describe the reconstructed structural brain connectome – i.e., a comprehensive description of the structural connections between brain regions (Jeurissen et al., 2017) – as a complex network. This allows describing brain network regarding characteristics such as integration and segregation using global and local graph theory metrics (Bullmore and Sporns, 2009; Rubinov and Sporns, 2010). These summary metrics, in turn, allow explaining functionalities of the brain that are not attributable to individual brain regions but rather emerge from the network as a whole (van den Heuvel and Sporns, 2013).

As far as we know, there is not published work in terms of characterizing PSP connectivity patterns by means of tractography and graph theory. In the present study, we reconstructed the structural connectome to detect the pathways of degeneration in PSP compared with healthy controls and their correlation with clinical features. Our hypothesis is that structural connectivity between cortical and deep gray matter structures is predominantly affected in PSP and that it correlates with characteristic clinical features of the disease. Furthermore, we assessed the potential discriminant ability of structural connectivity. We hypothesize that the rich information derived from the structural connectome has potential for distinguishing PSP patients from healthy controls with high accuracy. This will need to be further validated in larger cohorts encompassing the different PSP phenotypes.

2. Methods

2.1. Participants

Twenty-three probable PSP patients were recruited from the Parkinson's Disease and Movement Disorders Unit, Hospital Clínic de Barcelona. The inclusion criterion for PSP patients was the fulfillment of the NINDS-SPSP diagnostic criteria (Litvan et al., 1996a). The MDS PSP criteria (Höglinger et al., 2017) were retrospectively applied confirming that all patients also fulfilled them. The phenotype of each patient was also identified: 17 PSP presenting Richardson's syndrome (PSP-RS), 4 PSP with progressive gait freezing (PSP-PGF), 1 PSP resembling idiopathic Parkinson's disease (PSP-p) and 1 PSP presenting corticobasal syndrome (PSP-CBS). Twenty healthy controls (HC) matched by age, gender and years of education to PSP patients were recruited from patients' spouses or friends who volunteered to participate in the study and from the Institut de l'Envelliment, Universitat Autònoma de Barcelona.

Exclusion criteria consisted of: [1] pathological MRI findings other than mild white matter (WM) hyperintensities or suggestive of alternative diagnoses in patients, [2] MRI movement artifacts, [3] significant neurological, systemic or psychiatric comorbidity and [4] Mini-Mental State Examination scores < 25 or dementia in healthy participants.

Two PSP patients were excluded for excessive movement during the MR scan. One PSP patient was excluded for MR artifacts and another patient for a brain lesion in the right hemisphere. The final sample therefore consisted of 20 HC and 19 PSP patients (15 PSP-RS, 2 PSP-PGF, 1 PSP-p and 1 PSP-CBS). Sociodemographic and clinical characteristics of the groups are shown in Table 1. Concretely, from the 4 non PSP-RS patients, 2 started as an atypical phenotype (PSP-p and PSP-PGF) but progressed to a more richardsonian phenotype at follow-up. Given that most patients were PSP-RS, differences between phenotypes could not be considered in the main analyses. However, complementarily, we performed additional connectivity and classification analyses considering only PSP patients with Richardson's phenotype.

Table 1
Sociodemographic and clinical characteristics by group.

	HC (n = 20)	PSP (n = 19)	Stat/ p
Age	73.65 (5.7)	74.79 (7.4)	T = 0.543/p = .910
Years of education	9.9 (3.7)	7.4 (4.3)	T = 1.648/p = .120
Sex (male/female)	10/10	12/7	χ^2 = 0.686/p = .408
MMSE	29.05 (1.1)	23.19 (4.67)	T = 5.437/p < .001*
Years of evolution (yrs.)	–	4.16 (2.03)	–
H&Y (1:2:3:4:5)	–	0:1:8:5:5	–
PSPRS	–	37.42 (10.08)	–
FAB **	–	10.29 (2.67)	–

HC: healthy controls; PSP: Progressive supranuclear palsy patient group; MMSE: Mini-mental state examination; H&Y: Hoehn and Yahr scale; PSPRS: Progressive Supranuclear Palsy Rating Scale; FAB: Frontal Assessment Battery

* refers to significant results; Stats refers to Student's t-test (T) or Pearson's chi-square (χ^2).

** PSP patients with FAB scale n = 14.

Motor disease severity in PSP patients was evaluated using the Hoehn and Yahr (H&Y) and the PSP Rating Scale (PSPRS) (Hoehn and Yahr, 1967, Golbe and Ohman-Strickland, 2007) and executive dysfunction was assessed with the Frontal Assessment Battery (FAB) (Dubois et al., 2000). The study was approved by the Ethics Committee of the University of Barcelona and the Hospital Clinic (IRB00003099 and HCB/2015/0798, respectively). All participants provided written informed consent to participate after full explanation of the procedures involved.

2.2. MRI acquisition

MRI data were acquired with a 3 T scanner (MAGNETOM Trio, Siemens, Germany). The scanning protocol included high-resolution 3-dimensional T1-weighted images acquired in the sagittal plane (TR = 2300 ms, TE = 2.98 ms, TI = 900 ms, 240 slices, FOV = 256 mm; 1 mm isotropic voxel), two sets of single band spin-echo diffusion weighted images in the axial plane with opposite (anterior-posterior and posterior-anterior) phase encoding directions (TR = 7700 ms, TE = 89 ms, FOV = 244 mm; 2 mm isotropic voxel; number of directions = 30, b-value = 1000 s/mm^2, b_0 value = 0 s/mm^2) and a T2-weighted axial FLAIR sequence (TR = 9000 ms, TE = 96 ms).

2.3. MRI preprocessing

Structural MRI preprocessing was performed using the automated FreeSurfer pipeline (version 5.1; available at: https://surfer.nmr.mgh.harvard.edu/). Independent steps were performed: removal of non-brain tissue, automated Talairach transformation, intensity normalization (Sled et al., 1998), tessellation of the gray matter/white matter boundary, automated topology correction (Segonne et al., 2007), and accurate surface deformation to optimally place the gray matter/white matter and gray matter/cerebrospinal fluid boundaries (Fischl and Dale, 2000). The output of each step was visually inspected to guarantee correct and accurate preprocessing. The cerebral cortex was

parcellated into gyral and sulcal structures allowing the calculation of surface area measures and deep gray matter volumes were obtained from the automated FreeSurfer segmentation step (Filipek et al., 1994; Seidman et al., 1997; Fischl and Dale, 2000).

DWI images were preprocessed with FSL (version 5.08, available at: https://fsl.fmrib.ox.ac.uk/fsl), concretely using the FDT (FMRIB's Diffusion Toolbox), a toolbox that includes tools for data processing, local diffusion modelling and tractography (Jbabdi et al., 2012). Visual inspection was initially performed to identify motion-related and intensity artifacts in the DWI images. The preprocessing steps included brain extraction using BET, susceptibility-induced distortion correction using topup, and eddy-current distortion and subject motion correction with eddy. After preprocessing, images were thoroughly inspected to guarantee their quality.

2.4. Regions of interest

Sixty-eight cortical regions and 18 deep gray matter (DGM) structures derived from the Desikan-Killiany Atlas (Desikan et al., 2006) and the automated FreeSurfer segmentation atlas (Filipek et al., 1994; Seidman et al., 1997; Fischl and Dale, 2000) were selected as regions of interest (ROIs). Supplementary Tables 1A and 1B show the list of cortical and deep gray matter ROIs, respectively. Additionally, the volumetric information of each subcortical ROI was extracted, which is often used as an atrophy marker.

In order to use these ROIs as seeds for the tractography analysis, they were linearly registered from native structural space to native diffusion space with FSL's Flirt (Jenkinson and Smith, 2001; Jenkinson et al., 2002). To ensure that ROI masks did not overlap with each other after registration due to resample blur, each voxel was uniquely assigned to the mask for which it had the highest value, i.e., to which it had the highest probability of membership.

2.5. Tract-based spatial statistics

Voxel-wise statistical analysis of FA was carried out using TBSS (Tract-Based Spatial Statistics)(Smith et al., 2006). All subjects' FA data were aligned into a common space and then a mean FA image was calculated and thinned to generate a mean FA skeleton, representing the centers of all white matter tracts common to the group. Each subject's FA maps was then projected onto this skeleton and the resulting FA skeleton images were fed into a general lineal model. The same steps were employed to obtain the MD maps.

2.6. Brain network computation

The probability distribution of fiber directions in each voxel was calculated with Bedpostx (Behrens et al., 2007). Bedpostx runs Markov Chain Monte Carlo sampling to build up distributions on diffusion parameters at each voxel. Probtrackx (Behrens et al., 2007) was used to estimate probabilistic connectivity between seeds, as it repeatedly samples from the voxel-wise principal diffusion direction probability distribution calculated in Bedpostx, creating a new streamline at each iteration (Zhan et al., 2015). Five-thousand samples were generated for each seed mask, building a distribution on the likely tract location and path. A reconstructed streamline, or “fiber”, was considered to connect two ROIs if it intersected both. The number of reconstructed streamlines (NOS) between each pair of ROIs was taken as the strength of structural connectivity between these regions. This process was repeated for all cortical and deep gray matter ROI pairs, to compute an 86×86 connectivity matrix. To reduce the risk of false-positive connections, streamlines intersecting fewer than two regions were ignored, and only connections between pairs of regions that were detected in at least 50% of the individuals were considered (Zalesky et al., 2016).

2.7. Characterization of structural connectivity

In order to test for intergroup differences in interregional NOS between PSP and HC, we used TFNBS (Baggio et al., 2018), which performs statistical inference on brain graphs. This approach combines network-based statistics (Zalesky et al., 2010), frequently used for statistical analysis of brain graphs, and threshold-free cluster enhancement, a common method in voxel-wise statistical inference (Smith and Nichols, 2009). One of the main characteristics of TFNBS is that it allows generating edge-wise significance values that can be used to select relevant connectivity features. Control of the false discovery rate to 5% (FDR) was used to correct for multiple comparisons.

2.8. Graph theory computation

The analysis of structural connectivity was complemented with topological information derived from graph theory, allowing a description of global (whole-brain) and local (nodal) properties of the network (Bullmore and Sporns, 2009; Rubinov and Sporns, 2010). Our network consisted of 86 nodes (cortical and deep gray matter ROIs) connected to each other by a set of edges - i.e., the number of streamlines between them. The Brain Connectivity Toolbox (BCT) was used to extract the topological parameters, including global and local clustering coefficient, global and local node degree, small worldness, path length, local efficiency and betweenness centrality (See Rubinov and Sporns, 2010 for detailed definitions and calculations of the graph metrics included in this work).

2.9. Basic statistical analyses and clinical correlates

Intergroup comparisons of demographic, clinical, volumetric and connectivity variables were performed with the general linear model using in-house MATLAB scripts. Statistical significance was established through the Monte Carlo simulations with 10,000 permutations. Two-tailed p-values were calculated as the proportion of values in the null distribution more extreme than those observed in the actual model. FDR was then used to control for multiple comparisons. Given that the number of streamlines have a wide distribution depending on the tracts, Z-scores were calculated. Spearman correlations between clinical and imaging variables were evaluated using SPSS-24 (2016; Armonk, NY: IBM Corp.).

2.10. Classification procedure

Beyond testing for intergroup differences in structural connectivity, we were interested in assessing the usefulness of these connectivity measures in discriminating between PSP patients and HC using a supervised learning algorithm.

In order to select the most important features in an unbiased fashion, a mixed feature selection method was used for dimensionality reduction. A first set of features was selected with an intergroup comparison with TFNBS; i.e., connections whose p values were smaller than the significance threshold (0.05) were kept. Then, a based recursive feature elimination (RFE) method was adopted to select the optimal features to be introduced into the classifier. For the classification procedure, we used a logistic regression (LR) with L2 regularization, performed with the LR function from scikit-learn (http://scikit-learn.org), implemented in Python. LR parameters were optimized by cross-validated grid-search over a parameter grid. In order to avoid circularity in the classification, both feature selection and classification were implemented within a leave-one-out cross-validation (LOOCV). LOOCV takes one subject for testing whereas the remaining N-1 subjects are used for training the feature selection and classification algorithm. This method prevents overfitting, enhances the generalization power of the classifier, and returns an almost unbiased estimate of the probability of test error of the classification as the test subject is not included when

selecting significant features or defining parameters in any training step (Luntz, 1969).

To evaluate the performance of the classification procedure, we calculated its accuracy (number of subjects correctly classified as PSP patients or HC divided by total number of subjects), sensitivity (number of PSP patients correctly classified divided by the total number of PSP patients), and specificity (number of HC correctly classified divided by the total number of HC).

3. Results

3.1. Subjects

Table 1 shows the sociodemographic and clinical characteristics of the groups. No significant intergroup differences were observed for age, gender and years of education ($p = 0.910$, $p = 0.408$ and $p = 0.120$, respectively). A significant effect was found between groups in MMSE scores ($p < 0.001$).

3.2. Structural connectivity analysis

Fig. 1 shows the 41 connections with significantly different number of streamlines (NOS) between groups (all $p < 0.05$, FDR corrected). To test whether these edges displayed a predominant intra/inter-regional distribution or whether they were homogeneously distributed across the brain, we labeled them according to the regions connected (frontal, temporal, cingulate, parietal, occipital and deep gray matter (DGM) structures; see Supplementary Tables 2 and 3). From the 41 connections, 10 (24.4%) were found to be cortico-cortical tracts, 28 (68.3%) were cortico-DGM tracts and three (7.3%) DGM-DGM tracts (see Fig. 2 for further details). Concretely, fronto-DGM connections were predominantly reduced in PSP compared with healthy controls. No connections showed significantly higher NOS in PSP patients compared with HC.

3.3. Network graph metrics

As shown in Table 2 and Fig. 3, no group effect was found in global graph parameters when considering the whole-brain network.

At the node-level (Table 2), reduced nodal degree was observed in PSP patients compared with healthy controls in the bilateral hippocampus, the right frontal pole, and the right pars opercularis and left pars triangularis of the inferior frontal gyrus. For the sake of simplicity, given that many ROIs are considered, we only presented the regions

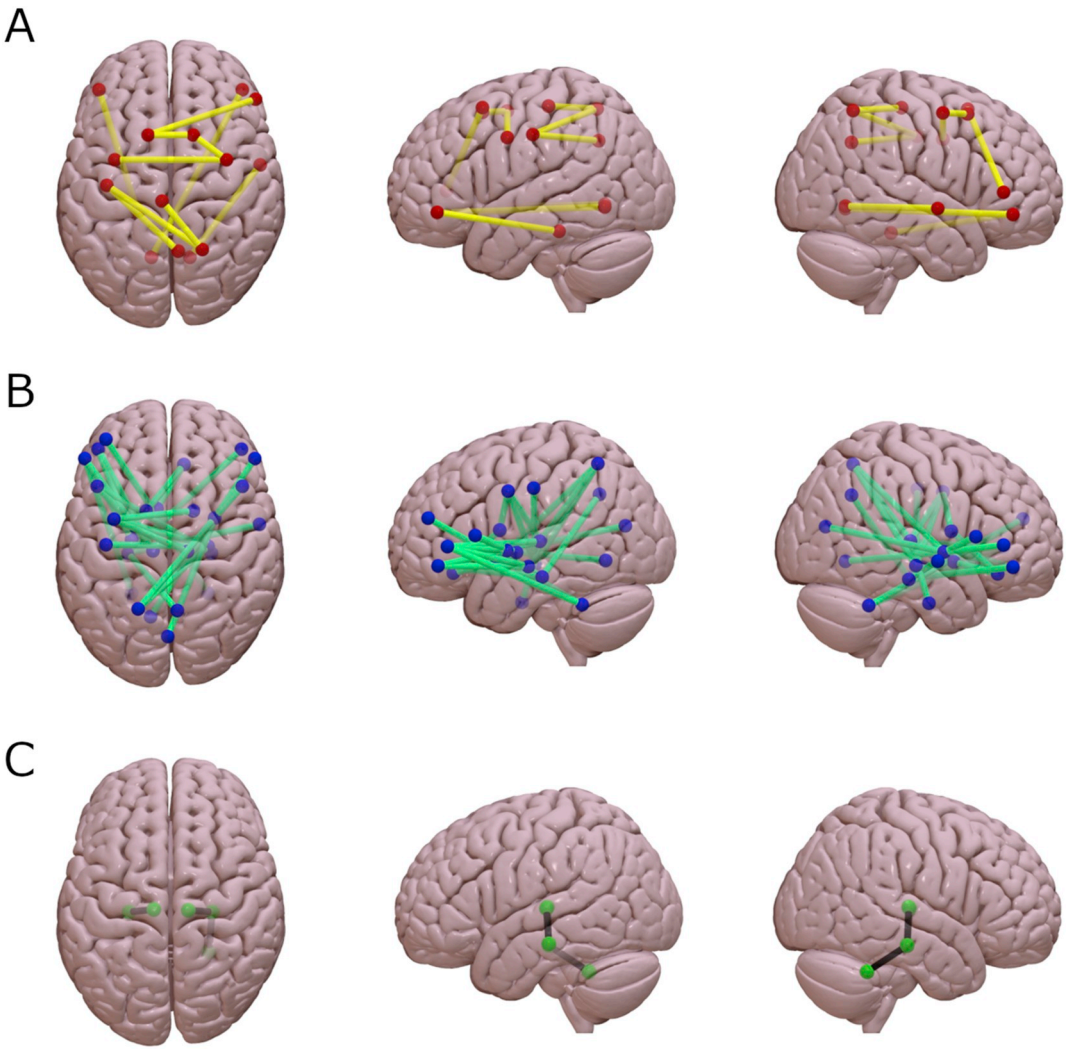

Fig. 1. Schematic representation of the 41 structural connections with reduced structural connectivity strength in progressive supranuclear palsy patients compared with healthy controls using threshold-free network based statistics.
A. Connectivity differences between groups in cortico-cortical tracts ($p < 0.05$, FDR corrected). B. Connectivity differences between groups in cortico-deep gray matter tracts ($p < 0.05$, FDR corrected). C. Connectivity differences between groups in deep gray matter-deep gray matter tracts ($p < 0.05$, FDR corrected). Connectivity figures were drawn using Surf Ice (www.nitrc.org).

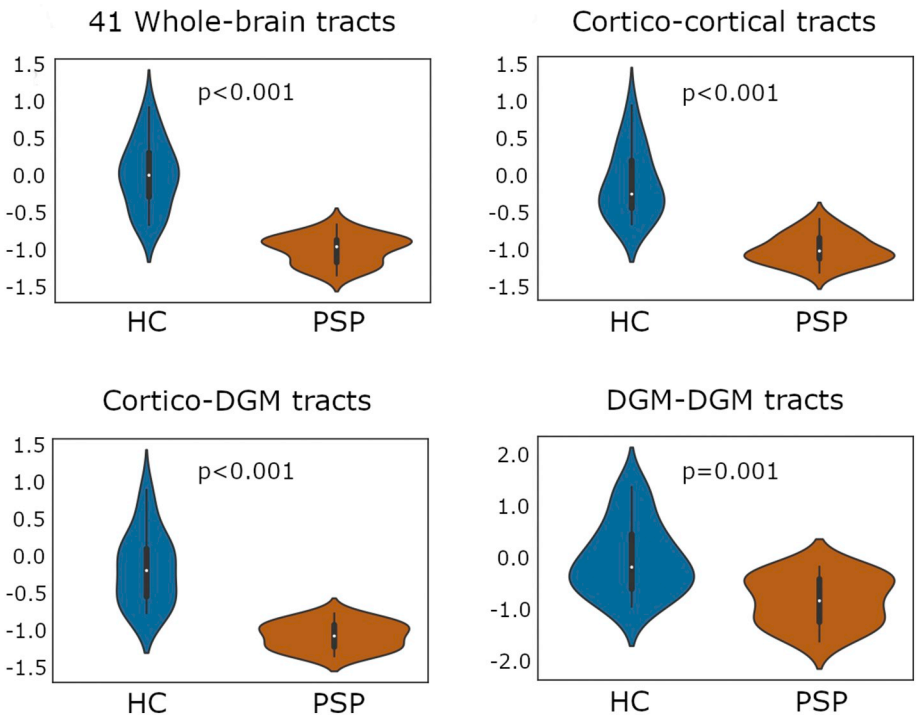

Fig. 2. Comparison of mean connectivity between progressive supranuclear palsy patients and healthy controls.
Plots illustrate the distribution of the measures of average number of streamlines (NOS) between cortical and deep gray matter connections derived from the 41 significantly reduced tracts found in PSP patients using threshold-free network based statistics (TFNBS). NOS values were Z-transformed to allow better comparability. Significance of intergroup analyses ($p < 0.05$, FDR corrected) are shown. HC: healthy controls; PSP: Progressive Supranuclear Palsy group; DGM: deep gray matter structures.

Table 2A
Whole-brain global graph measures by group.

	HC (n = 20)	PSP (n = 19)	Stat/ p
Modularity	0.5197 (0.013)	0.5205 (0.158)	T = 0.17697/p = .8536
Clustering coefficient	1.4638 (0.103)	1.5223 (0.122)	T = 1.62437/p = .2020
Nodal degree	68.295 (2.367)	66.668 (2.960)	T = 1.09038/p = .2025
Small Worldness	1.301 (0.083)	1.3446 (0.10)	T = 1.48381/p = .2025
Path Length	1.1247 (0.016)	1.1318 (0.015)	T = 1.39841/p = .2025

HC: healthy controls; PSP: Progressive supranuclear palsy patient group; Stats refers to Student's t-test (T).

and metrics found significant in local graph metrics.

Given the predominant reduced NOS in frontal and DGM connections previously found, we decided to complementarily study the fronto-DGM network. In this subnetwork, PSP patients showed a reduced global degree (GD) and an increase in global clustering (GC) and small worldness (SW) (Table 3, Fig. 4). Locally, reduced nodal degree was found in the bilateral hippocampus, the amygdala, the pallidum, the putamen, the nucleus accumbens, the thalamus, the ventral diencephalon and the cerebellum in the right hemisphere, and in cortical areas including the pars opercularis and pars triangularis of the inferior frontal gyrus, the frontal pole, the right precentral gyrus and the left rostral middle frontal gyrus (Table 3). Additionally, the other subnetworks – temporal-DGM, parietal-DGM and occipital-DGM – were also evaluated, showing no significant intergroup effect (see Supplementary tables 4).

Plots illustrate the distribution of the nodal degree, clustering coefficient, path length, small worldness and modularity in the fronto-deep gray matter subnetwork between groups. Significance of intergroup analyses ($p < 0.05$, FDR corrected) are shown. HC: healthy controls; PSP: progressive supranuclear palsy group.

3.4. TBSS analysis

TBSS showed abnormal values of FA and MD in PSP patients compared with HC. Concretely, reduced FA was predominantly detected in the corpus callosum, cerebellar peduncles, bilateral anterior and superior corona radiata, bilateral superior longitudinal fasciculus and bilateral posterior thalamic radiation (Supplementary fig. 1A). Complementary, increased MD was found in the corpus callosum, fornix, bilateral anterior and superior corona radiata and bilateral posterior thalamic radiation (Supplementary fig. 1B). No regions showed decreased FA or increased MD in HC compared with PSP patients.

3.5. Correlation analyses

As described above, decreased structural connectivity was found in PSP patients compared with healthy controls. To assess the clinical relevance of this finding, significant results were then correlated with frontal assessment battery (FAB) scores and the PSP Rating scale (PSPRS) in the PSP group.

The mean NOS of the 41 significant connections identified through TFNBS negatively correlated with the PSPRS scale ($r = -0.685$, $p = 0.001$). We then separated the mean NOS in cortico-cortical tracts, cortico-DGM tracts and DGM-DGM tracts to assess the presence of specific effects in interregional connections. The correlation between structural connectivity and PSPRS scale was found in cortico-DGM tracts and DGM-DGM tracts (respectively, $r = -0.626$, $p = 0.002$ and $r = -0.557$, $p = 0.007$). Mean NOS in DGM-DGM tracts significantly correlated with years of evolution ($r = -0.433$, $p = 0.032$). The correlation between DGM-DGM NOS and PSPRS scale remained significant when including years of evolution as a covariate ($r = -0.498$, $p = 0.018$). As the strongest effects seemed to be predominantly driven by cortico-DGM tracts and PSP is known to cause frontal lobe atrophy,

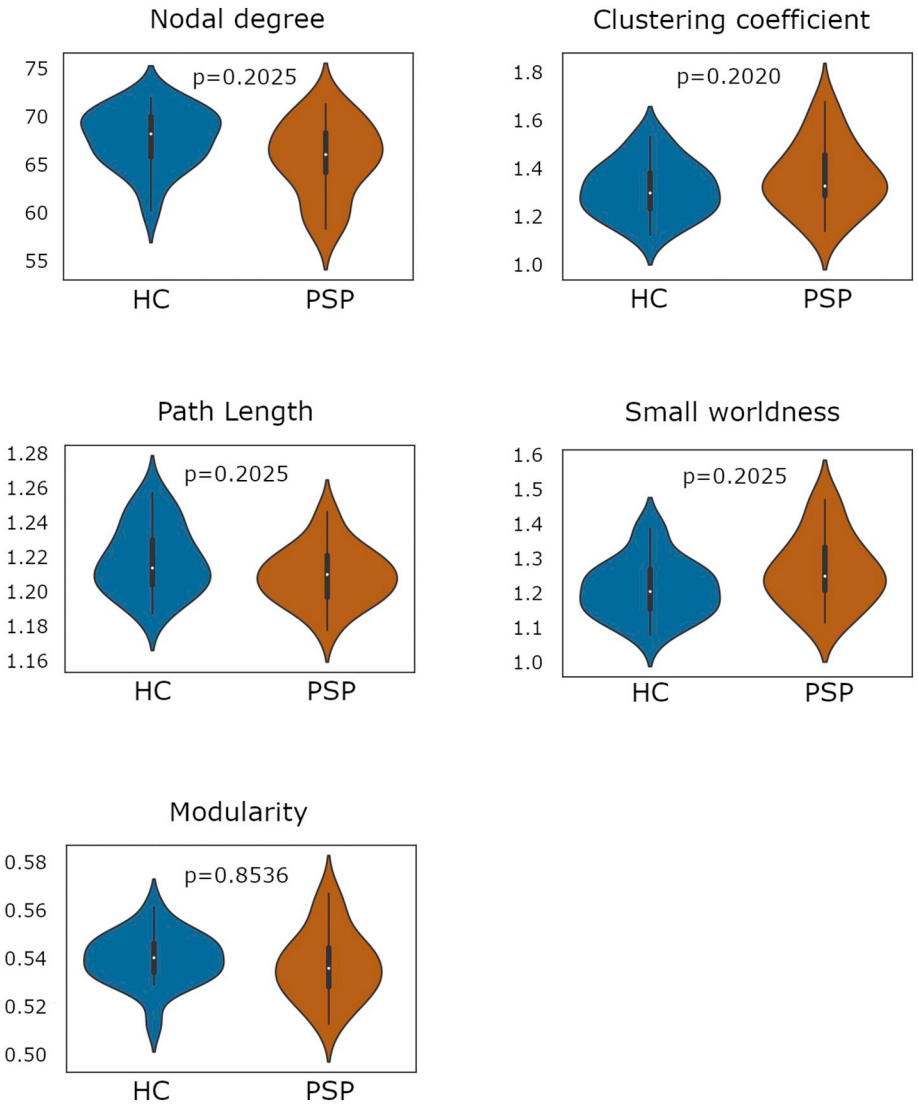

Fig. 3. Comparison of whole-brain global graph metrics between progressive supranuclear palsy patients and healthy controls.
Plots illustrate the distribution of the nodal degree, clustering coefficient, path length, small worldness and modularity in the whole-brain network between groups. Significance of intergroup analyses ($p < 0.05$, FDR corrected) are shown. HC: healthy controls; PSP: progressive supranuclear palsy group.

Table 2B
Significant whole-brain local graph measures by group.

	HC (n = 20)	PSP (n = 19)	Stat/ p
Local nodal degree			
Left Pars Triangularis	68.15 (3.631)	62.89 (6.35)	$T = 3.193/p = .0378$*
Right Pars Opercularis	55.7 (3.31)	48.74 (6.682)	$T = 4.156/p = .0086$*
Right Frontal pole	53.25 (2.845)	45.26 (7.385)	$T = 4.500/p = .0115$*
Left Hippocampus	81.05 (2.064)	76.63 (4.153)	$T = 4.241/p = .0086$*
Right Hippocampus	79.65 (1.496)	76.16 (5.315)	$T = 2.825/p = .0378$*

HC: healthy controls; PSP: Progressive supranuclear palsy patient group
* significant FDR corrected results; Stats refers to Student's t-test (T).

we then focused on fronto-DGM tracts. In this case, we found a correlation between these tracts and both the PSPRS scale and FAB scores ($r = -0.546$, $p = 0.008$ and $r = 0.543$, $p = 0.022$, respectively). A summary of these results can be found in Fig. 5. Additionally, clinical parameters were also correlated with whole-brain and fronto-DGM graph metrics, but no significant results were observed.

3.6. DGM volume analysis

Volume reductions were found in eight DGM structures, including the bilateral putamen, pallidum, thalamus, nucleus accumbens, ventral diencephalon, cerebellum and brainstem (Supplementary table 5). Furthermore, significant correlation results were detected between PSPRS and brainstem ($r = -0.67$ and $p = .001$) and right ventral diencephalon ($r = -0.56$, $p = .008$) volumes, and between FAB and bilateral hippocampus ($r = 0.56$, $p = .023$; $r = 0.62$, $p = .012$) and left nucleus accumbens ($r = 0.87$, $p < .001$) volumes.

3.7. Classification procedure results

The LR classification algorithm correctly predicted overall group membership with an accuracy of 82.23%, with 94.74% sensitivity and 70% specificity. As the leave-one-out cross-validation (LOOCV) scheme was used, the features selected in each iteration could differ slightly. The 41 structural connections that showed significant group effects when using the whole sample were obtained in > 85% of the iterations. Therefore, these connections seem to be stable in the feature selection procedure. Additionally, considering PSP subtypes, the only patient wrongly classified exhibited mixed PSP-PGF/PSP-RS characteristics.

Table 3A
Global graph measures in the fronto-DGM network by group.

	HC (n = 20)	PSP (n = 19)	Stat/ p
Modularity	0.4826 (0.021)	0.481 (0.025)	T = 0.23688/p = .8116
Clustering coefficient	1.608 (0.045)	1.210 (0.072)	T = 2.57015/p = .014*
Nodal degree	33.862 (0.793)	32.750 (1.186)	T = 3.45983/p = .005*
Small Worldness	1.087 (0.037)	1.129 (0.059)	T = 2.68864/p = .014*
Path Length	1.068 (0.017)	1.0718 (0.023)	T = 0.585108/p = .69725

HC: healthy controls; PSP: Progressive supranuclear palsy patient group; DGM: Deep gray matter structures
* refers to FDR corrected results; Stats refers to Student's t-test (T).

3.8. PSP-RS subtype results

Results, shown as Supplementary data, revealed predominance of cortico-DGM reductions in PSP-RS patients, correlating with PSPRS scores, and reductions of global degree in the fronto-DGM subnetwork. Furthermore, the classification procedure achieved an overall accuracy of 85%, with 100% sensitivity and 75% specificity.

4. Discussion

In this work, reduced structural connectivity was observed in PSP patients compared with HC. Concretely, reductions were predominantly detected in tracts linking frontal lobe regions and DGM structures, correlating with clinical scales of PSP. Furthermore, we found evidence that measures of structural connectivity might be useful to differentiate between PSP patients and HC with satisfactory accuracy.

Diffusion tensor imaging has been widely used to explore diffusion changes in PSP. When evaluating the integrity of white matter tracts, previous studies have measured different diffusion tensor-derived parameters, such as fractional anisotropy (FA) and mean diffusivity (MD), in specific regions of interest, or have performed whole-brain analyses with tract based statistics (TBSS). Diffusion abnormalities were predominantly reported in white matter tracts such as the corpus callosum, the fornix, the corona radiata, anterior and posterior thalamic

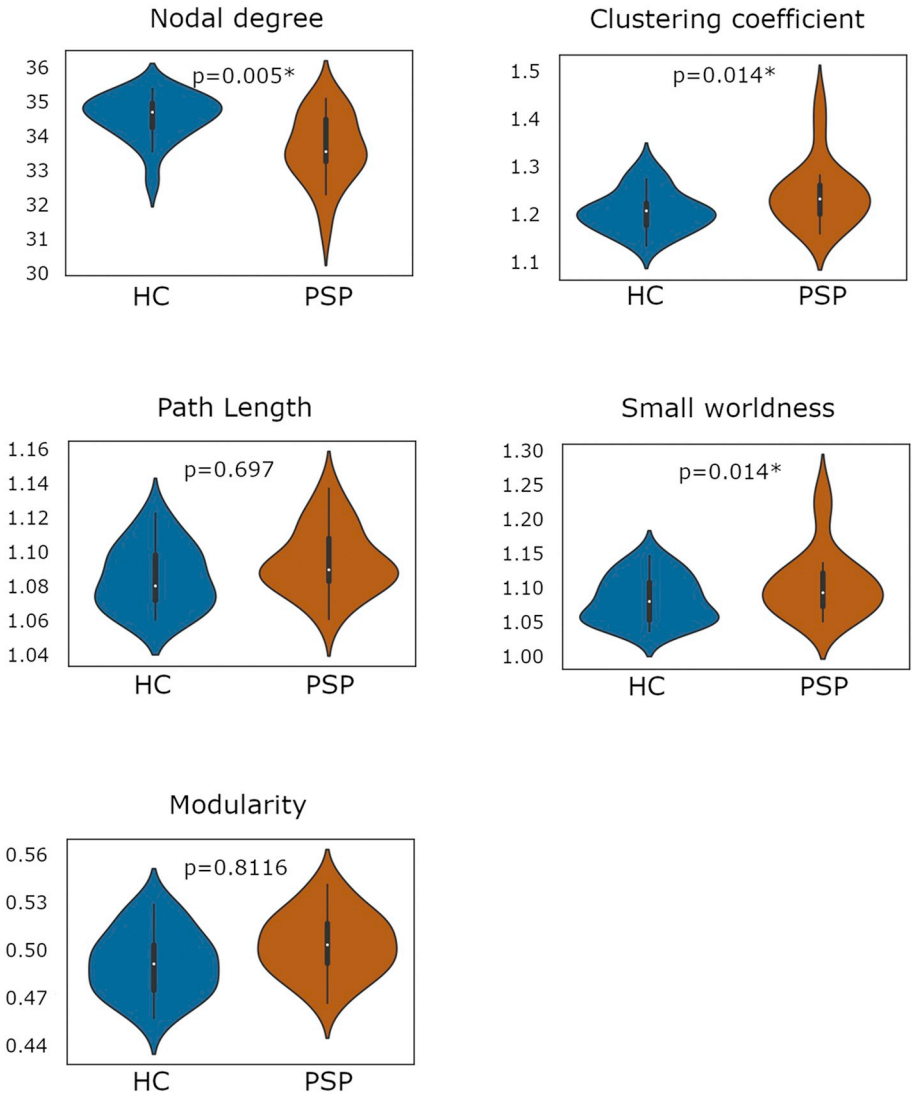

Fig. 4. Comparison of global graph metrics between progressive supranuclear palsy patients and healthy controls in the fronto-deep gray matter subnetwork.

Table 3B
Significant local graph measures in the fronto-DGM network by group.

	HC (n = 20)	PSP (n = 19)	Stat/ p
Local nodal degree			
Left Frontal Pole	26.75 (0.91)	25.26 (2.684)	T = 2.341/p = .0337*
Right Frontal Pole	27.2 (0.834)	25.79 (1.584)	T = 3.506/p = .0080*
Left Pars Opercularis	29.75 (1.943)	27.21 (2.226)	T = 3.801/p = .0080*
Right Pars Opercularis	28.6 (1.536)	25.84 (3.354)	T = 3.330/p = .0060*
Left Pars Triangularis	34.15 (1.694)	31.37 (3.32)	T = 3.321/p = .0160*
Right Pars Triangularis	35 (1.892)	32.37 (3.499)	T = 2.942/p = .0234*
Left Rostral Middle Frontal	36.75 (1.743)	34.16 (3.219)	T = 3.149/p = .0160*
Right Precentral	29.9 (1.119)	28.16 (1.642)	T = 3.889/p = .0060*
Left Hippocampus	36.05 (1.05)	33.37 (2.833)	T = 3.959/p = .0060*
Right Hippocampus	35.65 (0.671)	33.47 (2.435)	T = 3.849/p = .0060*
Right Amygdala	32.75 (1.446)	30.84 (2.387)	T = 3.037/p = .0142*
Right Pallidum	38.85 (0.366)	38.26 (1.147)	T = 2.175/p = .0395*
Right Putamen	38.95 (0.224)	38.63 (0.496)	T = 2.609/p = .0357*
Right Nucleus Accumbens	27.95 (1.05)	26.63 (1.892)	T = 2.709/p = .0234*
Right VentralDC	39 (0)	38.63 (0.684)	T = 2.411/p = .0090*
Right Cerebellum	35.95 (0.887)	33.79 (2.72)	T = 3.371/p = .0090*

HC: healthy controls; PSP: Progressive supranuclear palsy patient group
* significant FDR corrected results; Stats refers to Student's t-test (T).

radiation, the superior and inferior longitudinal fasciculus, the cingulum and the corticospinal tracts (Padovani et al., 2006; Whitwell et al., 2011a, 2011b; Surova et al., 2013, 2015; Agosta et al., 2014; Worker et al., 2014), and in deep gray matter structures, including the midbrain, the thalamus, the hippocampus and the caudate nucleus (Padovani et al., 2006; Wang et al., 2010; Whitwell et al., 2011a; Tsukamoto et al., 2012; Surova et al., 2015). Few studies have used tractography to study white matter tracts in PSP (Agosta et al., 2014; Surova et al., 2015; Surova et al., 2013). In these analyses, tracts of interest were derived from the probability maps and then diffusion measures were extracted from them. Abnormal FA and MD values were found in PSP patients compared with healthy controls, indicating that white matter damage in these tracts was specific of PSP pathology.

In our study, we used tractography to reconstruct the structural connectome. To our knowledge, this is the first study characterizing white matter abnormalities in PSP through structural connectivity derived from tractography. When studying the brain by only describing its constituent parts, we are missing a key feature: how the different elements of the system (e.g. brain regions) interact. Abnormal interactions between brain regions have been shown to be associated with many neurodegenerative disorders (Sporns, 2013). Building the structural connectome allows assessing the disruption effect of neurodegenerative diseases on specific pathways and regions of the network in a way that is closer to our understanding of brain organization (Griffa et al., 2013). In the current work, we observed significant structural connectivity alterations in PSP. Decreased NOS in PSP patients compared with HC were predominantly found in cortico-DGM connections linking frontal areas to the basal ganglia, the ventral diencephalon, the thalamus, the hippocampus and the cerebellum. Abnormal inter and intrahemispheric connections were observed, with a slight predominance in interhemispheric streamlines. No regions showed reductions in structural connectivity in HC compared with PSP patients. These findings were also found when considering only PSP-RS patients.

It is worth noting that the predominant reduction of NOS between frontal and DGM structures was found using a whole-brain approach, with no a priori selection of tracts. This highlights the importance of fronto-DGM pathways disruption in the neuropathological basis and symptomatology of the disease. Furthermore, it relates not only to frontal areas and DGM structures but also to their interaction (Cummings, 1993; Litvan et al., 1996b; Cordato et al., 2005). The clinical manifestations of PSP are closely linked to defects in this circuitry, including apathy, impulsivity and frontal behavioral disturbances (Cordato et al., 2005; Bonelli and Cummings, 2007). Previous studies have observed the relation between frontal disturbances (mostly evaluated with the Frontal Assessment Battery (FAB) or the Frontal Behavioral Inventory (FBI)) and the degeneration of specific white matter tracts and atrophy in subregions of the frontal cortex and DGM structures (Cordato et al., 2005; Whitwell et al., 2011b; Agosta et al., 2014). Severity of the disease as assessed with the PSPRS scale has also been correlated with white matter abnormalities in PSP-related tracts and structures, such as superior and inferior longitudinal fasciculus, the corpus callosum, the thalamus and the cerebellar peduncles (Whitwell et al., 2011a; Agosta et al., 2014; Surova et al., 2015). Our results are in agreement with these findings, as we found correlations between FAB and PSPRS scores and fronto-DGM structural connectivity in PSP patients, which include specific structures in this pathology. As far as we know, the current work is the first study linking changes in structural connectivity assessed through tractography to clinical manifestations in PSP.

Given the volumetric results, it can be hypothesized that the reduced connectivity involving some of these structures and their correlation with clinical features might be explained by their atrophy. Based on these findings, it is difficult to speculate whether the loss of white matter structural connectivity involving DGM regions is secondary to primary gray matter damage and subsequent axonal degeneration, or whether the disease process involves white matter abnormalities directly. However, reduced connectivity between frontal regions and the caudate was also found, along with reduced node degree in the amygdala, both structures not showing volumetric atrophy. Thus, although DGM structures are clearly affected in PSP, structural connectivity can detect changes in regions not presenting detectable atrophy. Furthermore, abnormal FA and MD measures were predominantly observed in the cerebellar peduncles, corpus callosum, bilateral anterior and superior corona radiata, bilateral superior longitudinal fasciculus and bilateral posterior thalamic radiation, in agreement with previous studies (Padovani et al., 2006; Whitwell et al., 2011a, 2011b; Surova et al., 2013, 2015; Agosta et al., 2014; Worker et al., 2014). We hypothesized that the connectivity reductions found in this work might be reflecting the loss of integrity in white matter tracts, along with subcortical GM atrophy in PSP patients.

Characterizing the structural connectome through graph theory provides information about the organization of the network (Griffa et al., 2013). When considering the whole brain, a tendency of higher global clustering coefficient, path length and “small-worldness”, along with reduced global mean degree could be observed in PSP patients' networks, although no global metric reached statistical significance. At

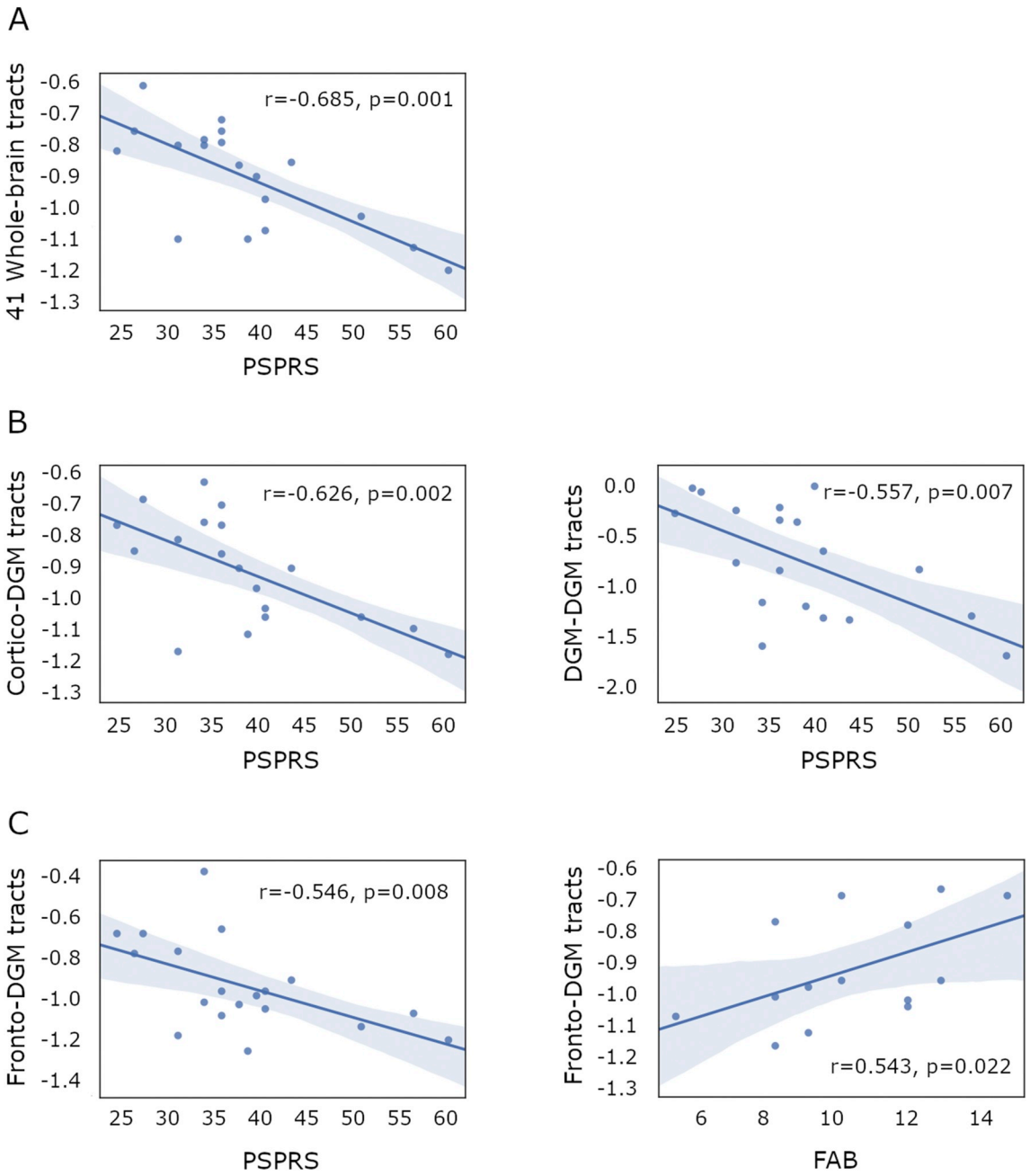

Fig. 5. Relationship between structural connectivity and clinical features in progressive supranuclear palsy patients.
A. Significant correlation between the mean NOS Z-score from the 41 reduced connections in PSP patients and the PSPRS scale. B. Significant correlation between the mean NOS Z-score from the cortico-DGM (left) and the DGM-DGM (right) reduced connections in PSP patients and the PSPRS scale. C. B. Significant correlation between the mean NOS Z-score from the fronto-DGM reduced connections in PSP patients and the PSPRS (left) and FAB (right) scales. NOS: number of streamlines; PSP: progressive supranuclear palsy group; DGM: deep gray matter structures.

the nodal level, reductions of nodal degree were found in the hippocampus, the frontal pole and the pars opercularis and triangularis of the inferior frontal gyrus. As previously mentioned, the involvement of frontal areas has been recurrently described in previous studies and it is related with the clinical manifestations of the disease. The hippocampus also seems to play a relevant role in PSP, as it was found to be involved in both reduced connections and abnormal whole-brain graph metrics in PSP patients. Deposits of phosphorylated tau protein is a hallmark of neurodegenerative tauopathies, such as PSP. Although the hippocampus is not primarily affected in this neuropathology, distinctive patterns of tau deposits were observed in previous studies (Milenkovic et al., 2014), as well as reduced volume in this structure (Saini et al., 2013; Wang et al., 2015). We hypothesize that these findings might explain the predominant abnormalities found in the hippocampus in PSP patients.

Given that no major group differences were identified in global measures, possibly due to the regional specificity of the disease-related alterations, we decided to specifically examine the fronto-DGM subnetwork, as it seemed to be predominantly affected in PSP. In the fronto-DGM network, PSP patients showed increased local interconnectedness manifested by higher measures of clustering and small-wordness, combined with a reduction of nodal degree, specifically in the bilateral hippocampus, the right amygdala, pallidum, putamen, nucleus accumbens, thalamus, ventral diencephalon and cerebellum, and in cortical areas including the pars opercularis and pars triangularis of the inferior frontal gyrus, the frontal pole, the right precentral gyrus

and the left rostral middle frontal gyrus. It is noteworthy that no significant results in global or local graph metrics were found in the other subnetworks. Therefore, these findings suggest that there might be a predominant reorganization of the network comprising frontal and DGM nodes in PSP patients compared with healthy controls.

The small world topology is thought to be a balance between local specialization and global integration when networks evolved from high complexity of dynamic behavior (Sporns et al., 2000). The alteration of the small-world architecture driven by increased clustering coefficient and path length has been reported in different neurological disorders, e.g. Alzheimer's disease (He et al., 2008; Lo et al., 2010; Yao et al., 2010), Parkinson's disease with mild cognitive impairment (Baggio et al., 2014; Galantucci et al., 2017) and schizophrenia (Zhang et al., 2012). In agreement with previous connectivity studies, it could be speculated that the increment in local clustering results from short-range connections, whereas the increased path length could imply a reduction of long-range connectivity and consequently a less effective communication within the pathological network in PSP patients. However, it is important to highlight that graph metrics results in neurodegenerative diseases are inconsistent, and that abnormal increases and decreases of small-word topology have been reported. E.g., studies in Alzheimer's disease observed decrease of small-word topology in these patients (Sanz-Arigita et al., 2010; Supekar et al., 2008), contrarily to the increase in small-word properties found in the previously mentioned studies (He et al., 2008; Lo et al., 2010; Yao et al., 2010). Some studies have looked into this aspect (Hallquist and Hillary, 2019; Tsai, 2018), showing that the reproducibility of network metrics can be affected by many factors, e.g., different sample sizes, how connectivity matrices are estimated (deterministic or probabilistic tractography in structural connectivity, full or partial correlation in functional connectivity), using binary or weighted matrices, the number of nodes in the network and the different thresholds applied on the connectivity matrices. These divergences in the methodology, along with different patient characteristics, can contribute to heterogeneous results, complicating the interpretability of graph metrics.

In the last few years, features extracted from different MRI modalities have been introduced into machine learning algorithms to assess their discriminant ability at the single-patient level in parkinsonian syndromes, commonly showing an accuracy around 80%, depending on the disease being evaluated (Focke et al., 2011; Filippone et al., 2012; Haller et al., 2012, 2013; Marquand et al., 2013; Nair et al., 2013; Cherubini et al., 2014; Salvatore et al., 2014; Huppertz et al., 2016; Péran et al., 2018; Baggio et al., 2019). Concretely, two previous studies specifically assessed the classification performance between PSP patients and HC (Focke et al., 2011; Salvatore et al., 2014). Focke and colleagues evaluated features from different modalities (T1, T2 and DTI), achieving a high accuracy of 94% when using diffusion measures from selected subcortical ROIs. Salvatore and colleagues described a whole-brain approach similar to our study. Principal component analysis (PCA) was used to reduce feature dimensionality of T1 images. The relevant features were then introduced into a classifier achieving an accuracy of 88.1%. To our knowledge, our work is the first study assessing the discrimination performance of structural connectivity in atypical parkinsonian patients. In PD patients, a study by Peña-Nogales and colleagues (2019) evaluated the ability of longitudinal structural connectivity to correctly distinguish PD patients from HC, obtaining an accuracy of 83.6%. As it can be shown, our results are in agreement with previous work using structural connectivity data as relevant features to distinguish parkinsonian patients at the single-subject level. It is noteworthy that only one PSP patient with mixed PSP-PGF/PSP-RS features was wrongly classified with the machine learning approach. We hypothesize that connectivity findings presented in this study might not only be linked exclusively to PSP-RS subtype. This idea should be further addressed with a larger sample inspecting possible connectivity differences within subtypes.

Some limitations to the present study should be pointed out. First, the PSP patient sample is relatively small; thus, we cannot assume that the set of structural connections identified in our study would generalize to other datasets. Future multicenter studies should be carried out to replicate our findings. Secondly, we lack confirmation of pathological diagnosis for the patients, which is the only approach that can fully confirm the PSP diagnosis and its subtypes. For this reason, we decided not to consider different PSP subtypes in the main analyses, as we were not able to confirm the subtype diagnosis with post-mortem evaluation. However, the machine learning results seems to indicate that there are no major structural connectivity differences between subtypes within the connections being evaluated in this study. The complementary analysis using only PSP patients with Richardson's syndrome showed similar findings. Nevertheless, in order to assess whether these results are mainly driven by the PSP-RS subtype, analyses need to be replicated with a larger sample of patients also encompassing the atypical PSP phenotypes. Thirdly, parcellations and tractography methodologies have a large impact on the characteristics of the reconstructed white matter tracts. Nonetheless, reduced integrity and atrophy of frontal regions and deep gray matter connections have been extensively reported in PSP in previous studies, supporting the validity of the results obtained in our work.

5. Conclusion

In this work, we demonstrated that modelling the brain as a structural connectome is a useful method to detect changes in the organization and topology of white matter tracts in PSP patients. Concretely, we found evidence that structural connectivity between frontal regions and deep gray matter structures is reduced in PSP patients compared with healthy controls and that disease's severity and executive dysfunction, measured by PSPRS and FAB scales respectively, are linked to these reductions in fronto-deep gray matter connections in PSP. Additionally, alteration of the small-world architecture implies that the topology of the network is altered, resulting in a less effective communication within the pathological network in PSP patients. Importantly, we showed for the first time that structural connectivity parameters have the potential to help distinguish between PSP patients and healthy controls at the single-subject level with high accuracy.

Funding

AA was supported by a 2016–2019 fellowship from the Departament d'Empresa i Coneixement de la Generalitat de Catalunya, AGAUR (2016FI_B 00360; 2017FI_B1 00013; 2018FI_B2 00001), AC was supported by APIF predoctoral fellowship from the University of Barcelona (2017–2018) and CU was supported by a fellowship from 2014, Spanish Ministry of Economy and Competitiveness (BES-2014-068173) and cofinanced by the European Social Fund (ESF). This study was sponsored by the Spanish Ministry of Economy and Competitiveness (PSI2013–41393-P; PSI2017–86930-P cofinanced by Agencia Estatal de Investigación (AEI) and the European Regional Development Fund), by Generalitat de Catalunya (2017SGR748) and by Fundació La Marató de TV3 in Spain (20142310; PI043296). MJM has received funding from Fondo de Investigaciones Sanitarias of Spain (FIS PI17/00096) and from Generalitat de Catalunya (AGAUR 2017SGR1502).

Disclosures

AA, HCB, BS, AC, CU, AG, AC_b, EM and CJ report no disclosures. MJM received honoraria for advice and lecture from Abbvie, Bial and Merzt Pharma and grants from Michael J. Fox Foundation for Parkinson's disease (MJFF): MJF_PPMI_10_001, PI044024. YC has received funding in the past 5 years from FIS/FEDER, H2020 programme Union Chimique Belge (UCB pharma), Teva, Medtronic, Abbvie, Novartis, Merz, Piramal Imaging, and Esteve, Bial and Zambon. YC is

currently associate editor of Parkisonism and Related Disorders.

Conflicts of interest

The authors report no conflicts of interest relevant to this study.

Appendix A. Supplementary data

Supplementary data to this article can be found online at https://doi.org/10.1016/j.nicl.2019.101899.

References

Agosta, F., Galantucci, S., Svetel, M., Lukić, M.J., Copetti, M., Davidovic, K., Tomić, A., Spinelli, E.G., Kostić, V.S., Filippi, M., 2014. Clinical, cognitive, and behavioural correlates of white matter damage in progressive supranuclear palsy. J. Neurol. 261, 913–924. https://doi.org/10.1007/s00415-014-7301-3.

Armstrong, M.J., 2018. Progressive Supranuclear palsy: an update. Curr. Neurol. Neurosci. Rep. 18, 12. https://doi.org/10.1007/s11910-018-0819-5.

Baggio, H.-C., Sala-Llonch, R., Segura, B., Marti, M.-J., Valldeoriola, F., Compta, Y., Tolosa, E., Junqué, C., 2014. Functional brain networks and cognitive deficits in Parkinson's disease. Hum. Brain Mapp. 35, 4620–4634. https://doi.org/10.1002/hbm.22499.

Baggio, H.C., Abos, A., Segura, B., Campabadal, A., Garcia-Diaz, A., Uribe, C., Compta, Y., Marti, M.J., Valldeoriola, F., Junque, C., 2018. Statistical inference in brain graphs using threshold-free network-based statistics. Hum. Brain Mapp. 39. https://doi.org/10.1002/hbm.24007.

Baggio, H.C., Abos, A., Segura, B., Campabadal, A., Uribe, C., Giraldo, D.M., Perez-Soriano, A., Muñoz, E., Compta, Y., Junque, C., Marti, M.J., 2019. Cerebellar resting-state functional connectivity in Parkinson's disease and multiple system atrophy: Characterization of abnormalities and potential for differential diagnosis at the single-patient level. NeuroImage Clin. 22, 101720.

Behrens, T.E.J., Berg, H.J., Jbabdi, S., Rushworth, M.F.S., Woolrich, M.W., 2007. Probabilistic diffusion tractography with multiple fibre orientations: what can we gain? Neuroimage 34, 144–155. https://doi.org/10.1016/j.neuroimage.2006.09.018.

Bonelli, R.M., Cummings, J.L., 2007. Frontal-subcortical circuitry and behavior. Dialogues Clin. Neurosci. 9, 141–151.

Boxer, A.L., Yu, J.-T., Golbe, L.I., Litvan, I., Lang, A.E., Höglinger, G.U., 2017. Advances in progressive supranuclear palsy: new diagnostic criteria, biomarkers, and therapeutic approaches. Lancet Neurol. 16, 552–563. https://doi.org/10.1016/S1474-4422(17)30157-6.

Brenneis, C., Seppi, K., Schocke, M., Benke, T., Wenning, G.K., Poewe, W., 2004. Voxel based morphometry reveals a distinct pattern of frontal atrophy in progressive supranuclear palsy. J. Neurol. Neurosurg. Psychiatry 75, 246–249.

Bullmore, E., Sporns, O., 2009. Complex brain networks: graph theoretical analysis of structural and functional systems. Nat. Rev. Neurosci. 10, 186–198. https://doi.org/10.1038/nrn2575.

Cherubini, A., Morelli, M., Nisticó, R., Salsone, M., Arabia, G., Vasta, R., Augimeri, A., Caligiuri, M.E., Quattrone, A., 2014. Magnetic resonance support vector machine discriminates between Parkinson disease and progressive supranuclear palsy. Mov. Disord. 29, 266–269.

Cordato, N.J., Halliday, G.M., Harding, A.J., Hely, M.A., Morris, J.G.L., 2000. Regional brain atrophy in progressive supranuclear palsy and Lewy body disease. Ann. Neurol. 47, 718–728. https://doi.org/10.1002/1531-8249(200006)47:6<718::AID-ANA4>3.0.CO;2-J.

Cordato, N.J., Pantelis, C., Halliday, G.M., Velakoulis, D., Wood, S.J., Stuart, G.W., Currie, J., Soo, M., Olivieri, G., Broe, G.A., Morris, J.G.L., 2002. Frontal atrophy correlates with behavioural changes in progressive supranuclear palsy. Brain 125, 789–800.

Cordato, N.J., Duggins, A.J., Halliday, G.M., Morris, J.G.L., Pantelis, C., 2005. Clinical deficits correlate with regional cerebral atrophy in progressive supranuclear palsy. Brain 128, 1259–1266. https://doi.org/10.1093/brain/awh508.

Cummings, J.L., 1993. Frontal-subcortical circuits and human behavior. Arch. Neurol. 50, 873–880.

Dąbrowska, M., Schinwelski, M., Sitek, E.J., Muraszko-Klaudel, A., Brockhuis, B., Jamrozik, Z., Sławek, J., 2015. The role of neuroimaging in the diagnosis of the atypical parkinsonian syndromes in clinical practice. Neurol. Neurochir. Pol. 49, 421–431. https://doi.org/10.1016/j.pjnns.2015.10.002.

Desikan, R.S., Ségonne, F., Fischl, B., Quinn, B.T., Dickerson, B.C., Blacker, D., Buckner, R.L., Dale, A.M., Maguire, R.P., Hyman, B.T., Albert, M.S., Killiany, R.J., 2006. An Automated Labeling System for Subdividing the Human Cerebral Cortex on MRI Scans into Gyral Based Regions of Interest. https://doi.org/10.1016/j.neuroimage.2006.01.021.

Dubois, B., Slachevsky, A., Litvan, I., Pillon, B., 2000. The FAB: a frontal assessment battery at bedside. Neurology 55, 1621–1626.

Filipek, P.A., Richelme, C., Kennedy, D.N., Caviness, V.S., 1994. The young adult human brain: an MRI-based morphometric analysis. Cereb. cortex (New York, N.Y.) 4, 344–360 (n.d.).

Filippone, M., Marquand, A.F., Blain, C.R.V., Williams, S.C.R., Mourão-Miranda, J., Girolami, M., 2012. Probabilistic prediction of neurological disorders with a statistical assessment of neuroimaging data modalities. Ann. Appl. Stat. 6, 1883–1905.

Fischl, B., Dale, A.M., 2000. Measuring the thickness of the human cerebral cortex from magnetic resonance images. Proc. Natl. Acad. Sci. 97, 11050–11055. https://doi.org/10.1073/pnas.200033797.

Focke, N.K., Helms, G., Pantel, P.M., Scheewe, S., Knauth, M., Bachmann, C.G., Ebentheuer, J., Dechent, P., Paulus, W., Trenkwalder, C., 2011. Differentiation of typical and atypical Parkinson syndromes by quantitative MR imaging. Am. J. Neuroradiol. 32, 2087–2092.

Galantucci, S., Agosta, F., Stefanova, E., Basaia, S., van den Heuvel, M.P., Stojković, T., Canu, E., Stanković, I., Spica, V., Copetti, M., Gagliardi, D., Kostić, V.S., Filippi, M., 2017. Structural brain connectome and cognitive impairment in Parkinson disease. Radiology 283, 515–525. https://doi.org/10.1148/radiol.2016160274.

Golbe, L.I., Ohman-Strickland, P.A., 2007. A clinical rating scale for progressive supranuclear palsy. Brain 130, 1552–1565. https://doi.org/10.1093/brain/awm032.

Griffa, A., Baumann, P.S., Thiran, J.-P., Hagmann, P., 2013. Structural connectomics in brain diseases. Neuroimage 80, 515–526. https://doi.org/10.1016/J.NEUROIMAGE.2013.04.056.

Haller, S., Badoud, S., Nguyen, D., Garibotto, V., Lovblad, K.O., Burkhard, P., 2012. Individual Detection of Patients with Parkinson Disease using Support Vector Machine Analysis of Diffusion Tensor Imaging Data: Initial Results. Am. J. Neuroradiol. 33, 2123–2128.

Hallquist, M.N., Hillary, F.G., 2019. Graph theory approaches to functional network organization in brain disorders: a critique for a brave new small-world. Netw. Neurosci. 3, 1–26. https://doi.org/10.1162/netn_a_00054.

He, Y., Chen, Z., Evans, A., 2008. Structural insights into aberrant topological patterns of large-scale cortical networks in Alzheimer's disease. J. Neurosci. 28, 4756–4766. https://doi.org/10.1523/JNEUROSCI.0141-08.2008.

Hoehn, M.M., Yahr, M.D., 1967. Parkinsonism: onset, progression and mortality. Neurology 17, 427–442. https://doi.org/10.1212/WNL.17.5.427.

Höglinger, G.U., Respondek, G., Stamelou, M., Kurz, C., Josephs, K.A., Lang, A.E., Mollenhauer, B., Müller, U., Nilsson, C., Whitwell, J.L., Arzberger, T., Englund, E., Gelpi, E., Giese, A., Irwin, D.J., Meissner, W.G., Pantelyat, A., Rajput, A., van Swieten, J.C., Troakes, C., Antonini, A., Bhatia, K.P., Bordelon, Y., Compta, Y., Corvol, J.-C., Colosimo, C., Dickson, D.W., Dodel, R., Ferguson, L., Grossman, M., Kassubek, J., Krismer, F., Levin, J., Lorenzl, S., Morris, H.R., Nestor, P., Oertel, W.H., Poewe, W., Rabinovici, G., Rowe, J.B., Schellenberg, G.D., Seppi, K., van Eimeren, T., Wenning, G.K., Boxer, A.L., Golbe, L.I., Litvan, I., 2017. Movement Disorder Society-endorsed PSP study group, 2017. Clinical diagnosis of progressive supranuclear palsy: the movement disorder society criteria. Mov. Disord. 32, 853–864. https://doi.org/10.1002/mds.26987.

Huppertz, H.-J., Möller, L., Südmeyer, M., Hilker, R., Hattingen, E., Egger, K., Amtage, F., Respondek, G., Stamelou, M., Schnitzler, A., Pinkhardt, E.H., Oertel, W.H., Knake, S., Kassubek, J., Höglinger, G.U., 2016. Differentiation of neurodegenerative parkinsonian syndromes by volumetric magnetic resonance imaging analysis and support vector machine classification. Mov. Disord. 31, 1506–1517.

Jbabdi, S., Sotiropoulos, S.N., Savio, A.M., Graña, M., Behrens, T.E.J., 2012. Model-based analysis of multishell diffusion MR data for tractography: how to get over fitting problems. Magn. Reson. Med. 68, 1846–1855. https://doi.org/10.1002/mrm.24204.

Jenkinson, M., Smith, S., 2001. A global optimisation method for robust affine registration of brain images. Med. Image Anal. 5, 143–156.

Jenkinson, M., Bannister, P., Brady, M., Smith, S., 2002. Improved optimization for the robust and accurate linear registration and motion correction of brain images. Neuroimage 17, 825–841.

Jeurissen, B., Descoteaux, M., Mori, S., Leemans, A., 2017. Diffusion MRI fiber tractography of the brain. NMR Biomed. e3785. https://doi.org/10.1002/nbm.3785.

Litvan, I., Agid, Y., Calne, D., Campbell, G., Dubois, B., Duvoisin, R.C., Goetz, C.G., Golbe, L.I., Grafman, J., Growdon, J.H., Hallett, M., Jankovic, J., Quinn, N.P., Tolosa, E., Zee, D.S., 1996a. Clinical research criteria for the diagnosis of progressive supranuclear palsy (Steele-Richardson-Olszewski syndrome): report of the NINDS-SPSP international workshop. Neurology 47, 1–9.

Litvan, I., Mega, M.S., Cummings, J.L., Fairbanks, L., 1996b. Neuropsychiatric aspects of progressive supranuclear palsy. Neurology 47, 1184–1189.

Lo, C.-Y., Wang, P.-N., Chou, K.-H., Wang, J., He, Y., Lin, C.-P., 2010. Diffusion tensor Tractography reveals abnormal topological Organization in Structural Cortical Networks in Alzheimer's disease. J. Neurosci. 30, 16876–16885. https://doi.org/10.1523/JNEUROSCI.4136-10.2010.

Looi, J.C.L., Macfarlane, M.D., Walterfang, M., Styner, M., Velakoulis, D., Lätt, J., van Westen, D., Nilsson, C., 2011. Morphometric analysis of subcortical structures in progressive supranuclear palsy: in vivo evidence of neostriatal and mesencephalic atrophy. Psychiatry Res. Neuroimaging 194, 163–175. https://doi.org/10.1016/j.pscychresns.2011.07.013.

Luntz, A., 1969. On estimation of characters obtained in statistical procedure of recognition. Tech. Kibern 7.

Marquand, A.F., Filippone, M., Ashburner, J., Girolami, M., Mourao-Miranda, J., Barker, G.J., Williams, S.C.R., Leigh, P.N., Blain, C.R.V., 2013. Automated, High Accuracy Classification of Parkinsonian Disorders: A Pattern Recognition Approach. PLoS One 8, e69237.

Milenkovic, I., Petrov, T., Kovacs, G.G., 2014. Patterns of Hippocampal Tau Pathology Differentiate Neurodegenerative Dementias. Dement. Geriatr. Cogn. Disord. 38, 375–388.

Nair, S.R., Tan, L.K., Mohd Ramli, N., Lim, S.Y., Rahmat, K., Mohd Nor, H., 2013. A decision tree for differentiating multiple system atrophy from Parkinson's disease using 3-T MR imaging. Eur. Radiol. 23, 1459–1466.

Padovani, A., Borroni, B., Brambati, S.M., Agosti, C., Broli, M., Alonso, R., Scifo, P., Bellelli, G., Alberici, A., Gasparotti, R., Perani, D., 2006. Diffusion tensor imaging and voxel based morphometry study in early progressive supranuclear palsy. J. Neurol. Neurosurg. Psychiatry 77, 457–463. https://doi.org/10.1136/jnnp.2005.075713.

Péran, P., Barbagallo, G., Nemmi, F., Sierra, M., Galitzky, M., Traon Le, A.P., Payoux, P.,

Meissner, W.G., Rascol, O., 2018. MRI supervised and unsupervised classification of Parkinson's disease and multiple system atrophy. Mov. Disord. 33, 600–608.
Price, S., Paviour, D., Scahill, R., Stevens, J., Rossor, M., Lees, A., Fox, N., 2004. Voxel-based morphometry detects patterns of atrophy that help differentiate progressive supranuclear palsy and Parkinson's disease. Neuroimage 23, 663–669. https://doi.org/10.1016/j.neuroimage.2004.06.013.
Quattrone, A., Nicoletti, G., Messina, D., Fera, F., Condino, F., Pugliese, P., Lanza, P., Barone, P., Morgante, L., Zappia, M., Aguglia, U., Gallo, O., 2008. MR imaging index for differentiation of progressive Supranuclear palsy from Parkinson disease and the Parkinson variant of multiple system atrophy. Radiology 246, 214–221. https://doi.org/10.1148/radiol.2453061703.
Rubinov, M., Sporns, O., 2010. Complex network measures of brain connectivity: uses and interpretations. Neuroimage 52, 1059–1069. https://doi.org/10.1016/J.NEUROIMAGE.2009.10.003.
Saini, J., Bagepally, B.S., Sandhya, M., Pasha, S.A., Yadav, R., Thennarasu, K., Pal, P.K., 2013. Subcortical structures in progressive supranuclear palsy: vertex-based analysis. Eur. J. Neurol. 20, 493–501. https://doi.org/10.1111/j.1468-1331.2012.03884.x.
Salvatore, C., Cerasa, A., Castiglioni, I., Gallivanone, F., Augimeri, A., Lopez, M., Arabia, G., Morelli, M., Gilardi, M.C., Quattrone, A., 2014. Machine learning on brain MRI data for differential diagnosis of Parkinson's disease and Progressive Supranuclear Palsy. J. Neurosci. Methods 222, 230–237.
Sanz-Arigita, E.J., Schoonheim, M.M., Damoiseaux, J.S., Rombouts, S.A.R.B., Maris, E., Barkhof, F., Scheltens, P., Stam, C.J., 2010. Loss of 'small-world' networks in Alzheimer's disease: graph analysis of fMRI resting-state functional connectivity. PLoS One 5, e13788. https://doi.org/10.1371/journal.pone.0013788.
Segonne, F., Pacheco, J., Fischl, B., 2007. Geometrically accurate topology-correction of cortical surfaces using nonseparating loops. IEEE Trans. Med. Imaging 26, 518–529. https://doi.org/10.1109/TMI.2006.887364.
Seidman, L.J., Faraone, S.V., Goldstein, J.M., Goodman, J.M., Kremen, W.S., Matsuda, G., Hoge, E.A., Kennedy, D., Makris, N., Caviness, V.S., Tsuang, M.T., 1997. Reduced subcortical brain volumes in nonpsychotic siblings of schizophrenic patients: a pilot magnetic resonance imaging study. Am. J. Med. Genet. 74, 507–514.
Sled, J.G., Zijdenbos, A.P., Evans, A.C., 1998. A nonparametric method for automatic correction of intensity nonuniformity in MRI data. IEEE Trans. Med. Imaging 17, 87–97. https://doi.org/10.1109/42.668698.
Smith, S.M., Nichols, T.E., 2009. Threshold-free cluster enhancement: addressing problems of smoothing, threshold dependence and localisation in cluster inference. Neuroimage 44, 83–98. https://doi.org/10.1016/j.neuroimage.2008.03.061.
Smith, S.M., Jenkinson, M., Johansen-Berg, H., Rueckert, D., Nichols, T.E., Mackay, C.E., Watkins, K.E., Ciccarelli, O., Cader, M.Z., Matthews, P.M., Behrens, T.E.J., 2006. Tract-based spatial statistics: Voxelwise analysis of multi-subject diffusion data. Neuroimage 31, 1487–1505. https://doi.org/10.1016/j.neuroimage.2006.02.024.
Sporns, O., 2013. Network attributes for segregation and integration in the human brain. Curr. Opin. Neurobiol. 23, 162–171. https://doi.org/10.1016/J.CONB.2012.11.015.
Sporns, O., Tononi, G., Edelman, G.M., 2000. Theoretical neuroanatomy: relating anatomical and functional connectivity in graphs and cortical connection matrices. Cereb. Cortex 10, 127–141.
Supekar, K., Menon, V., Rubin, D., Musen, M., Greicius, M.D., 2008. Network analysis of intrinsic functional brain connectivity in Alzheimer's disease. PLoS Comput. Biol. 4, e1000100. https://doi.org/10.1371/journal.pcbi.1000100.
Surova, Y., Szczepankiewicz, F., Lätt, J., Nilsson, M., Eriksson, B., Leemans, A., Hansson, O., van Westen, D., Nilsson, C., 2013. Assessment of global and regional diffusion changes along white matter tracts in parkinsonian disorders by MR Tractography. PLoS One 8. https://doi.org/10.1371/journal.pone.0066022.
Surova, Y., Nilsson, M., Lätt, J., Lampinen, B., Lindberg, O., Hall, S., Widner, H., Nilsson, C., van Westen, D., Hansson, O., 2015. Disease-specific structural changes in thalamus and dentatorubrothalamic tract in progressive supranuclear palsy. Neuroradiology 57, 1079–1091. https://doi.org/10.1007/s00234-015-1563-z.
Tsai, S.-Y., 2018. Reproducibility of structural brain connectivity and network metrics using probabilistic diffusion tractography. Sci. Rep. 8, 11562. https://doi.org/10.1038/s41598-018-29943-0.
Tsukamoto, K., Matsusue, E., Kanasaki, Y., Kakite, S., Fujii, S., Kaminou, T., Ogawa, T., 2012. Significance of apparent diffusion coefficient measurement for the differential diagnosis of multiple system atrophy, progressive supranuclear palsy, and Parkinson's disease: evaluation by 3.0-T MR imaging. Neuroradiology 54, 947–955. https://doi.org/10.1007/s00234-012-1009-9.
van den Heuvel, M.P., Sporns, O., 2013. Network hubs in the human brain. Trends Cogn. Sci. 17, 683–696. https://doi.org/10.1016/j.tics.2013.09.012.
Wang, J., Wai, Y., Lin, W.-Y., Ng, S., Wang, C.-H., Hsieh, R., Hsieh, C., Chen, R.-S., Lu, C.-S., 2010. Microstructural changes in patients with progressive supranuclear palsy: a diffusion tensor imaging study. J. Magn. Reson. Imaging 32, 69–75. https://doi.org/10.1002/jmri.22229.
Wang, G., Wang, J., Zhan, J., Nie, B., Li, P., Fan, L., Zhu, H., Feng, T., Shan, B., 2015. Quantitative assessment of cerebral gray matter density change in progressive supranuclear palsy using voxel based morphometry analysis and cerebral MR T1-weighted FLAIR imaging. J. Neurol. Sci. 359, 367–372.
Whitwell, J.L., Avula, R., Master, A., Vemuri, P., Senjem, M.L., Jones, D.T., Jack, C.R., Josephs, K.A., 2011a. Disrupted thalamocortical connectivity in PSP: a resting-state fMRI, DTI, and VBM study. Parkinsonism Relat. Disord. 17, 599–605. https://doi.org/10.1016/j.parkreldis.2011.05.013.
Whitwell, J.L., Master, A.V., Avula, R., Kantarci, K., Eggers, S.D., Edmonson, H.A., Jack, C.R., Josephs, K.A., 2011b. Clinical correlates of white matter tract degeneration in progressive Supranuclear palsy. Arch. Neurol. 68, 753–760. https://doi.org/10.1001/archneurol.2011.107.
Worker, A., Blain, C., Jarosz, J., Chaudhuri, K.R., Barker, G.J., Williams, S.C.R., Brown, R.G., Leigh, P.N., Dell'acqua, F., Simmons, A., 2014. Diffusion tensor imaging of Parkinson's disease, multiple system atrophy and progressive supranuclear palsy: a tract-based spatial statistics study. PLoS One 9. https://doi.org/10.1371/journal.pone.0112638.
Yao, Z., Zhang, Y., Lin, L., Zhou, Y., Xu, C., Jiang, T., Alzheimer's Disease Neuroimaging Initiative, 2010. Abnormal cortical networks in mild cognitive impairment and Alzheimer's disease. PLoS Comput. Biol. 6, e1001006. https://doi.org/10.1371/journal.pcbi.1001006.
Zalesky, A., Fornito, A., Bullmore, E.T., 2010. Network-based statistic: identifying differences in brain networks. Neuroimage 53, 1197–1207. https://doi.org/10.1016/j.neuroimage.2010.06.041.
Zalesky, A., Fornito, A., Cocchi, L., Gollo, L.L., van den Heuvel, M.P., Breakspear, M., 2016. Connectome sensitivity or specificity: which is more important? Neuroimage 142, 407–420. https://doi.org/10.1016/j.neuroimage.2016.06.035.
Zhan, L., Zhou, J., Wang, Y., Jin, Y., Jahanshad, N., Prasad, G., Nir, T.M., Leonardo, C.D., Ye, J., Thompson, P.M., for the Alzheimer's Disease Neuroimaging Initiative, 2015. Comparison of nine tractography algorithms for detecting abnormal structural brain networks in Alzheimer's disease. Front. Aging Neurosci. 7, 48. https://doi.org/10.3389/fnagi.2015.00048.
Zhang, Y., Lin, L., Lin, C.-P., Zhou, Y., Chou, K.-H., Lo, C.-Y., Su, T.-P., Jiang, T., 2012. Abnormal topological organization of structural brain networks in schizophrenia. Schizophr. Res. 141, 109–118. https://doi.org/10.1016/j.schres.2012.08.021.